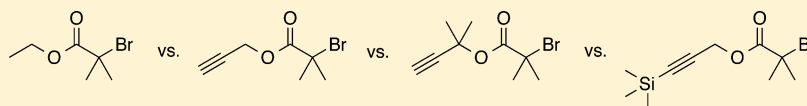


Prop-2-yn-1-yl 2-Bromo-2-methylpropanoate: Identification and Suppression of Side Reactions of a Commonly Used Terminal Alkyne-Functional ATRP Initiator

William K. Storms-Miller and Coleen Pugh*

Department of Polymer Science, The University of Akron, Akron, Ohio 44325-3909, United States

S Supporting Information



ABSTRACT: The atom transfer radical polymerization (ATRP) of styrene was investigated using the popular alkyne-functional initiator prop-2-yn-1-yl 2-bromo-2-methylpropanoate (PBIB). The polymerization kinetics and evolution of molecular weight as a function of monomer conversion were systematically studied with PBIB and similar initiators with protecting groups at the reactive propargylic and terminal acetylenic sites. These studies were compared to control studies using the nonfunctional initiator ethyl 2-bromoisobutyrate. As confirmed by NMR analysis of a model reaction, the terminal alkynes undergo oxidative alkyne–alkyne coupling under ATRP conditions, resulting in polymers with bimodal molecular weight distributions. This side reaction is significant because it diminishes the orthogonality of ATRP/copper-catalyzed azide–alkyne cycloaddition procedures as well as the control of ATRP.

INTRODUCTION

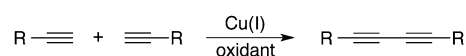
Atom transfer radical polymerization (ATRP) is a well-established and very popular polymerization method that enables the synthesis of diverse polymer architectures with well-controlled molecular weights and narrow molecular weight distributions.^{1,2} ATRP tolerates many functional groups, thereby facilitating the preparation of highly functionalized polymers.³ In addition to main-chain functional polymers prepared by the polymerization of functional monomers, telechelic polymers have been produced using functional initiators⁴ or by functionalization of the halogen chain end.⁵ Because of the functional group tolerance of ATRP and the rapid growth in the use of copper-catalyzed azide–alkyne cycloadditions (CuCAAC), ATRP has been used extensively to produce polymers with azide- and alkyne-functional groups, either at the chain ends^{6–10} or as pendant groups along the polymer backbone.^{11,12}

Although CuCAAC and radical polymerization chemistries are often treated as orthogonal, neither azides nor terminal alkynes are totally inert to radicals and/or the conditions used for radical polymerizations. For example, 2-azidoethyl methacrylate dimerizes to form a triazoline ring under reversible addition–fragmentation chain transfer (RAFT) polymerization conditions, even at relatively low temperature (50 °C).¹³ Similarly, alkyl azides undergo a 1,3-dipolar cycloaddition with many electron-deficient olefins, such as *N*-isopropylacrylamide, dimethylacrylamide, methyl acrylate, and methyl methacrylate, under RAFT polymerization conditions, to form triazoles and aziridines.¹⁴

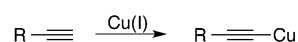
As outlined in Scheme 1, terminal alkynes participate in a variety of reactions, including oxidative alkyne–alkyne coupling,^{15–17,17} formation of cuprous acetylides,¹⁸ radical

Scheme 1. Known Side Reactions of Terminal Alkynes That May Occur under ATRP Conditions

A) oxidative coupling



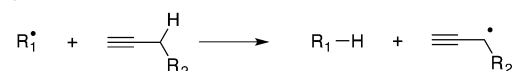
B) cuprous acetylide formation



C) radical addition



D) radical chain transfer



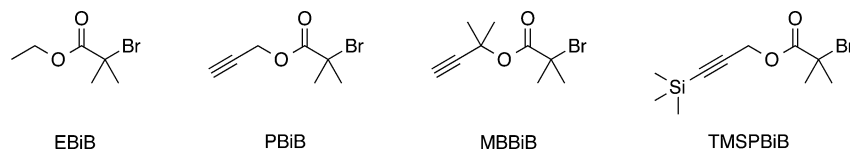
addition across the triple bond,¹⁹ and chain transfer of the radical with propargylic atoms,²⁰ under conditions that may exist in conventional and/or “controlled” radical polymerizations. Alkyne-functional monomers also participate in side reactions during radical polymerizations that result in cross-

Received: April 1, 2015

Revised: May 13, 2015

Published: June 1, 2015

Scheme 2. Control Initiator, Ethyl 2-Bromoisobutyrate (EBiB), and Alkyne-Functional Initiators Used in This Study: Prop-2-yn-1-yl 2-Bromo-2-methylpropanoate (PBiB), 2-Methylbut-3-yn-2-yl 2-Bromo-2-methylpropanoate (MBBiB), and 3-(Trimethylsilyl)prop-2-yn-1-yl 2-Bromo-2-methylpropanoate (TMSPBiB)



linked polymers,^{11,21,22} which necessitates the use of low temperature²³ and/or protection of the terminal acetylenic site.^{12,24} Nevertheless, alkyne-functionalized ATRP initiators and RAFT chain-transfer agents have been used extensively, with these known side reactions mostly ignored or dismissed due to the intrinsically low concentration of the resulting chain ends. Occasionally the acetylenic position of terminal alkyne-functionalized ATRP initiators and RAFT chain-transfer agents are protected using a silicon-protecting group in order to prevent “copper complexation”²⁵ or cuprous acetylide formation and other unspecified “side reactions”^{8,26–29}

This paper investigates the possible side reactions involving one of the most popular alkyne-functional ATRP initiators, prop-2-yn-1-yl 2-bromo-2-methylpropanoate (PBiB), by comparing its ATRP polymerization of styrene to that of an analogous initiator without an alkyne group, ethyl 2-bromoisobutyrate (EBiB), as the control (Scheme 2). These results are further compared to the ATRP polymerizations of styrene initiated by alkyne-functional initiators that have protecting groups at either the propargylic position (2-methylbut-3-yn-2-yl 2-bromo-2-methylpropanoate = MBBiB) or the terminal acetylenic site (3-(trimethylsilyl)prop-2-yn-1-yl 2-bromo-2-methylpropanoate = TMSPBiB). We then offer a route to suppress the side reactions of alkyne-functional initiators in order to prepare highly functional polystyrenes with controlled molecular weights and narrow molecular weight distributions.

EXPERIMENTAL SECTION

Materials. Anisole (Aldrich, 99.7%), benzene-*d*₆ (Cambridge Isotopes, 99.5%), 2-bromoisobutyryl bromide (Aldrich, 98%), cupric bromide (Aldrich, 99%), and 4-(dimethylamino)pyridine (Aldrich, 99%) (DMAP) were used as received. Cuprous bromide (Alfa Aesar, 98%) was stirred with acetic acid, washed with diethyl ether, and dried under vacuum. Diethyl ether (Fischer) was distilled from purple sodium benzophenone ketyl. Ethyl 2-bromoisobutyrate (Aldrich, 98%) was distilled under reduced pressure. Reagent grade methylene chloride was dried over CaH₂ and distilled. 2-Methyl-3-butyn-2-ol (Aldrich, 98%) was dried over 4 Å molecular sieves and distilled. *N,N,N',N''*-Pentamethyldiethylenetriamine (Aldrich, 99%) (PMDETA) was dried over K₂CO₃ and distilled under reduced pressure. Propargyl acetate was synthesized in 57% yield by esterification of acetyl chloride with propargyl alcohol (Supporting Information). Prop-2-yn-1-yl 2-bromo-2-methylpropanoate³⁰ (PBiB) and 3-(trimethylsilyl)propargyl alcohol³¹ were synthesized according to literature procedures. Styrene (Aldrich, 99%) was passed through basic alumina and distilled from CaH₂ under reduced pressure. Reagent grade tetrahydrofuran (THF) was distilled from purple sodium benzophenone ketyl. Triethylamine (Aldrich, 99%) was dried over KOH and distilled.

Techniques. All reactions were performed under a N₂ atmosphere using a Schlenk line unless noted otherwise. The kinetic experiments for the polymerizations were performed in triplicate in 20 mL screw-capped vials, which were assembled in a Vacuum Atmospheres drybox under a N₂ atmosphere. The monomer conversions were measured by ¹H NMR spectroscopy by following the changes in the integral of the

β -vinyl resonances (5.23 and 5.75 ppm) of styrene relative to that of the methoxy resonance (3.80 ppm) of anisole, which was used as an internal standard. ¹H (300 or 500 MHz) and ¹³C NMR (75 or 125 MHz) NMR spectra (δ , ppm) were recorded on either a Varian Mercury 300 spectrometer or a Varian 500 spectrometer, respectively. 2-D NMR spectra were recorded on the Varian 500 spectrometer. Unless noted otherwise, all spectra were recorded in CDCl₃, and the resonances were measured relative to residual solvent resonances and referenced to tetramethylsilane (0.0 ppm).

Number-average (M_n) and weight-average (M_w) molecular weights relative to linear polystyrene (GPC_{pst}) and polydispersities ($D = M_w/M_n$) were determined by gel permeation chromatography (GPC) from calibration curves of log M_n vs elution volume at 35 °C using THF as solvent (1.0 mL/min), a guard column and a set of 50, 100, 500, and 10⁴ Å as well as linear (50–10⁴ Å) Styragel 5 μ m columns, a Waters 486 tunable UV/Vis detector set at 254 nm, a Waters 410 differential refractometer, and Millenium Empower 3 software. All samples were passed through basic activated alumina to remove copper catalysts prior to injection into the GPC.

Synthesis of 2-Methylbut-3-yn-2-yl 2-Bromo-2-methylpropanoate (MBBiB). Because of the steric hindrance of both the electrophile and nucleophile, a large excess of the nucleophile was used, including as the solvent for the addition, to increase the rate of reaction. A solution of 2-bromoisobutyryl bromide (2.0 mL, 16 mmol) in 2-methyl-3-butyn-2-ol (5 mL, 50 mmol) was slowly added dropwise to an ice-cooled solution of DMAP (0.18 g, 1.5 mmol) and triethylamine (2.3 mL, 17 mmol) in 2-methyl-3-butyn-2-ol (5 mL, 50 mmol). The reaction mixture was stirred at room temperature for 22 h and then concentrated by rotary evaporation. The concentrate was diluted with CH₂Cl₂ (20 mL) and washed sequentially with 1.5 M aqueous HCl (10 mL), saturated aqueous NaHCO₃ (10 mL), and saturated aqueous NaCl (10 mL), and then dried over MgSO₄. After filtration and removing the solvent by rotary evaporation, the crude product was distilled, collecting the fraction boiling at 75–77 °C/10 mmHg to yield 2.1 g (56%) of 2-methylbut-3-yn-2-yl 2-bromo-2-methylpropanoate as a colorless oil. ¹H NMR (300 MHz): 1.72 (s, C(CH₃)₂O), 1.92 (s, C(CH₃)₂Br), 2.56 (s, HCC). ¹³C NMR (75 MHz): 28.6 (C(CH₃)₂O), 30.7 (C(CH₃)₂Br), 56.6 (C(CH₃)₂Br), 72.9 (HCC), 73.3 (C(CH₃)₂O), 84.1 (HCC), 169.7 (C=O).

Synthesis of 3-(Trimethylsilyl)prop-2-yn-1-yl 2-Bromo-2-methylpropanoate (TMSPBiB). A solution of 2-bromoisobutyryl bromide (2.3 mL, 0.19 mol) in diethyl ether (5 mL) was added dropwise over 30 min to an ice-cooled solution of 3-(trimethylsilyl)prop-2-yn-1-ol (2.0 g, 0.16 mol) and triethylamine (1.6 g, 0.15 mol) in diethyl ether (10 mL). The reaction mixture was stirred at room temperature for 23 h. Precipitated triethylammonium bromide was removed by filtration through a fritted glass funnel, and the solvent was removed from the filtrate by rotary evaporation. The orange residue was distilled (55–57 °C/1 mmHg), and the resulting orange distillate was passed through a plug of basic activated alumina using hexanes/ethyl acetate (10:1) as the eluant to remove residual 2-bromoisobutyric acid. Solvent was removed by rotary evaporation and then by drying under vacuum on a Schlenk line to yield 3.1 g (72%) of TMSPBiB as a colorless oil. ¹H NMR (500 MHz): 0.19 (s, Si(CH₃)₃), 1.96 (s, CBr(CH₃)₂), 4.76 (s, CH₂). ¹³C NMR (125 MHz): –0.2 (Si(CH₃)₃), 30.9 (CBr(CH₃)₂), 54.4 (CH₂), 55.3 (CBr(CH₃)₂), 92.9 (SiCC), 98.4 (SiCC), 171.0 (C=O).

Reaction of Prop-2-yn-1-yl 2-Bromo-2-methylpropanoate with the ATRP Catalyst System in the Absence of Monomer. A solution of PBiB (60 mg, 0.30 mmol) and PMDETA (56 mg, 0.32

Table 1. Polymerization Results from the Atom Transfer Radical Polymerizations of Styrene (St) at 110 °C Using the 2-Bromoisobutyrate Initiators Shown in Scheme 2^a

initiator	corresponding to Figure 1				corresponding to Figure 2			corresponding to Figures 5 and 6		
	time (min)	max conv	\bar{D}	$k_p^{\text{app}} \times 10^4 \text{ (s}^{-1}\text{)}$	M_n/p (kDa)	R^2	f^{app} (%)	M_p/p (kDa)	R^2	
EBiB	239	77	1.16 ± 0.01	1.00 ± 0.03	13.4 ± 0.4	0.98	78 ± 4			
PBiB	327	83	1.46 ± 0.03	0.931 ± 0.05	10.8 ± 2.3	0.63	96 ± 22 ^b	low M_p high M_p	16.7 ± 0.6 29.5 ± 1.0	0.98 0.98
MBBiB	343	87	1.35 ± 0.04	0.988 ± 0.02	20.4 ± 0.6	0.97	51 ± 8		27.7 ± 1.6	0.96
TMSPBiB	367	87	1.24 ± 0.02	1.10 ± 0.07	13.9 ± 0.6	0.97	75 ± 5		19.2 ± 0.9	0.97

^a[St]:[I]:[CuBr]:[CuBr₂]:[PMDETA] = 100:1:1:0.1:1.1; PMDETA = *N,N,N',N',N''*-pentamethyldiethylenetriamine; \bar{D} = polydispersity = M_w/M_n at the maximum conversion listed; k_p^{app} = the apparent rate constants of propagation from the least-squares fits (slopes) of the data in Figure 1; M_n/p are the slopes from the data in Figure 2, in which p = monomer conversion; R^2 = the coefficient of determination for the statistical fits of the data in Figures 2, 5 and 6; f^{app} = the apparent initiator efficiency from the data in Figure 2; M_p/p are the slopes from the data in Figures 5 and 6, in which M_p is the peak molecular weight. ^bThis initiator efficiency is based on M_n for the entire bimodal molecular weight distribution.

mmol) in benzene-*d*₆ (3.0 g) in a Schlenk tube was degassed by three freeze–pump–thaw cycles (5–10–5 min), and the Schlenk tube was backfilled with nitrogen. After removing an aliquot (1.0 mL) with a syringe, the remaining solution was added via a syringe to a mixture of CuBr (44 mg, 0.31 mmol) and CuBr₂ (7.1 mg, 32 μmol) under a N₂ atmosphere. The reaction mixture was stirred at 25 °C, and aliquots (1.0 mL) were removed with a syringe after 35 and 75 min. The aliquots were passed through a plug of basic activated alumina to remove the catalyst and were analyzed by ¹H NMR spectroscopy.

Model Reaction of Propargyl Acetate with the ATRP Catalyst System. A solution of propargyl acetate (35 mg, 36 μmol) and PMDETA (68 mg, 39 μmol) in benzene-*d*₆ (3.83 g) was degassed by three freeze–pump–thaw cycles (5–10–5 min) and then taken into the drybox. This solution was added to a mixture of CuBr (49 mg, 0.34 mmol) and CuBr₂ (8 mg, 4 μmol) in a 20 mL vial, and the mixture was stirred rapidly at room temperature for 30 min. An aliquot (1.0 mL) of the mixture was transferred to each of four 20 mL vials. The vials were capped and the screw caps were sealed to the vial with electrical tape. The vials were removed from the drybox and three vials were immersed in an oil bath at 85 °C. The reaction mixtures were stirred at 85 °C and then removed from the oil bath at 1, 2.5, and 16.5 h, for comparison to the time 0 sample. These vials were cooled to room temperature and exposed to the atmosphere to quench the catalyst. The samples were filtered through a plug of basic activated alumina and analyzed by ¹H and ¹³C NMR spectroscopy.

Styrene Polymerizations: Kinetic Studies. The kinetic experiments were performed in triplicate. In a typical procedure, a stock solution of PMDETA (3.8 mL, 1.2 mmol; 0.27 g PMDETA/5.0 mL anisole solution) was added by syringe to a solution of ethyl 2-bromoisobutyrate (0.21 mg, 1.1 mmol) in styrene (11 g, 0.11 mol) in a 100 mL Schlenk tube equipped with a magnetic stir bar and sealed with a rubber septum. This solution was degassed by three freeze–pump–thaw cycles (5–15–5 min) and then taken into the drybox. The contents of the Schlenk tube were added to a mixture of CuBr (0.16 g, 1.1 mmol) and CuBr₂ (26 mg, 0.12 mmol), and the resulting mixture was stirred rapidly at room temperature for 30 min. An aliquot (1.0 mL) of the polymerization mixture was transferred by syringe to each of fifteen 20 mL vials. The vials were capped, and the screw caps were sealed to the vial with electrical tape. The vials were removed from the drybox and immersed in an oil bath at 110 °C. The polymerization mixtures were stirred at 110 °C and then removed from the oil bath in groups of three at five time intervals. These vials were cooled in an ice bath to stop the reaction and exposed to atmosphere to quench the catalyst.

The polymerizations were analyzed by ¹H NMR spectroscopy to determine monomer concentration ($[M]$) and conversion at time t , and the kinetic parameters (eqs 1 and 2), in which R_p is the rate of polymerization, k_p is the rate constant of propagation, $[P^*]$ is the concentration of growing chains, and k_p^{app} is the apparent rate constant of propagation.

$$R_p = \frac{-d[M]}{dt} = k_p[P^*][M] \quad (1)$$

$$\ln \frac{[M]_0}{[M]} = k_p[P^*]t = k_p^{\text{app}}t \quad (2)$$

The polymerizations were also analyzed by GPC to determine the molecular weight data, initiator efficiency (f) and apparent initiator efficiency (f^{app}) according to eqs 3 and 4,³² in which p is the extent of reaction, M_n^{theo} is the theoretical number-average molecular weight based on the ratio of the amounts of monomer and initiator reacted, and M_n^{obs} is the observed M_n .

$$M_n = p \frac{[M]_0}{f[I]_0} \times MW_{\text{monomer}} \quad (3)$$

$$f^{\text{app}} = \frac{[P]}{[I]_0} = \frac{M_n^{\text{theo}}}{M_n^{\text{obs}}} \quad (4)$$

RESULTS AND DISCUSSION

Kinetics of Styrene Polymerization. Table 1 summarizes the polymerization results for the ATRP polymerizations of styrene at 110 °C using the control initiator and the three alkyne-functionalized initiators shown in Scheme 2. This data corresponds to the first-order monomer conversion plots presented in Figure 1 and the plots of molecular weight vs conversion presented in Figures 2, 5, and 6. All of the polymerizations reached high conversions (77–87%) in 4–6 h, and the semilogarithmic kinetic plots are linear throughout the polymerizations. As summarized in Table 1, the apparent rate constants ($k_p^{\text{app}} = (0.931\text{--}1.10) \times 10^{-4} \text{ s}^{-1}$) using the alkyne initiators are identical within experimental error to that of the control initiator ($(1.00 \pm 0.03) \times 10^{-4} \text{ s}^{-1}$). Therefore, functionalization of the ATRP initiator with a terminal alkyne group or protected alkyne or propargylic groups does not result in greater termination than that detected in the control experiment with a nonalkyne initiator.

Figure 2 plots the number-average molecular weights of the polystyrenes produced as a function of monomer conversion for the same ATRP polymerizations analyzed in Figure 1. The data for the PBiB-initiated polymerization are quite scattered ($R^2 = 0.63$) and nonlinear. As summarized in Table 1, the molecular weight distributions are relatively broad ($\bar{D} = 1.31\text{--}1.46$) at all conversions; the GPC chromatograms in Figure 3 demonstrate that these molecular weight distributions are bimodal. When the two peak molecular weights (M_p) of the bimodal distributions are plotted as a function of monomer conversion (Figure 4), both relationships are linear, which

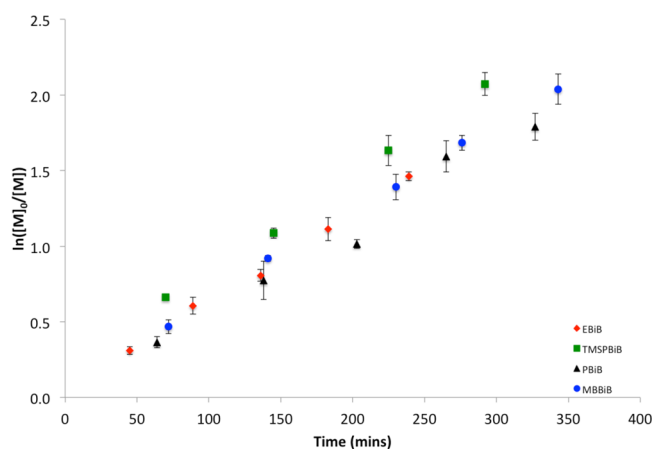


Figure 1. First-order monomer conversions in the atom transfer radical polymerization of styrene (St) at 110 °C using the 2-bromoisobutyrate initiators shown in Scheme 2 and N,N,N',N'',N'' -pentamethyldiethylenetriamine (PMDETA) as the ligand; $[St]:[I]:[CuBr]:[CuBr_2]:[PMDETA] = 100:1:1:0.1:1.1$; the error bars correspond to one standard deviation from triplicate experiments.

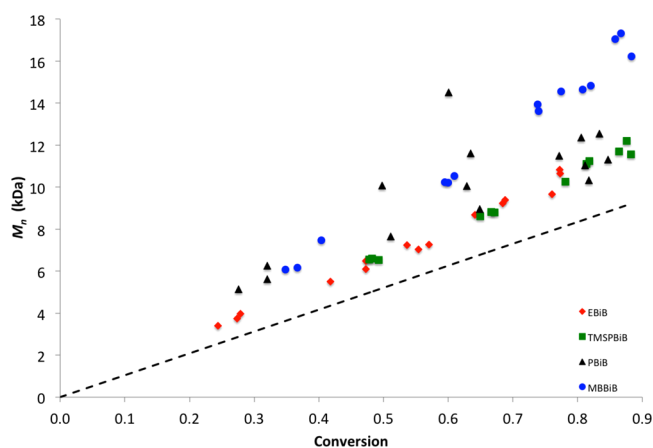


Figure 2. Number-average molecular weight (M_n) as a function of monomer conversion for the atom transfer radical polymerizations of styrene (St) at 110 °C using the 2-bromoisobutyrate initiators shown in Scheme 2 and N,N,N',N'',N'' -pentamethyldiethylenetriamine (PMDETA) as the ligand; $[St]:[I]:[CuBr]:[CuBr_2]:[PMDETA] = 100:1:1:0.1:1.1$. The theoretical molecular weight (dashed line) was calculated as $\text{conversion} \times [M]_0/[I]_0 \times 104.15$.

demonstrates that chain transfer is not detectable. On average, the peak molecular weights of the higher molecular weight distributions are 1.8 times higher than those of the lower molecular weight peaks (Table 1). The bimodal molecular weight distributions and linear first-order kinetics are consistent with a nondegenerative chain coupling reaction. However, the higher molecular weight distributions can not be attributed to termination by radical–radical coupling since the first-order kinetic plots are linear and therefore do not detect termination and because there is a bimodal molecular weight distribution at all conversions, not just at the end of the polymerization. The amount of coupled chains also varies from sample to sample and with monomer conversion, creating the large scatter in the M_n vs conversion plot in Figure 2.

One of the known sites for side reactions of alkynes under radical polymerization conditions is at the propargylic position (Scheme 1D); chain transfer of a propargylic hydrogen atom is favored by resonance stabilization of the resulting propargylic

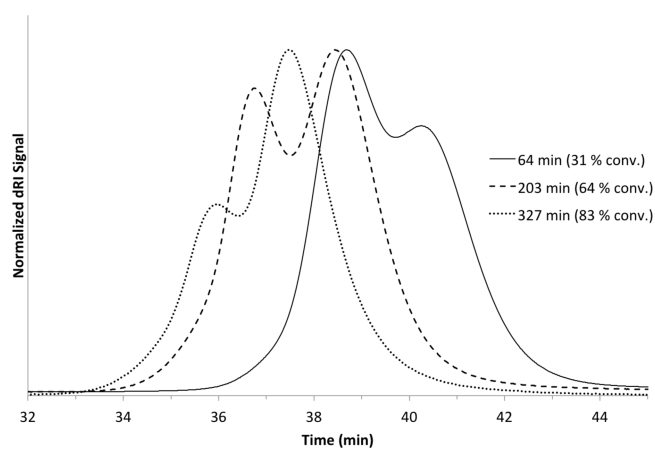


Figure 3. Representative GPC chromatograms of polystyrene initiated from prop-2-yn-1-yl 2-bromo-2-methylpropanoate (PBiB) at 110 °C at 64, 203, and 327 min using N,N,N',N'',N'' -pentamethyldiethylenetriamine (PMDETA) as the ligand; $[St]:[PBiB]:[CuBr]:[CuBr_2]:[PMDETA] = 100:1:1:0.1:1.1$.

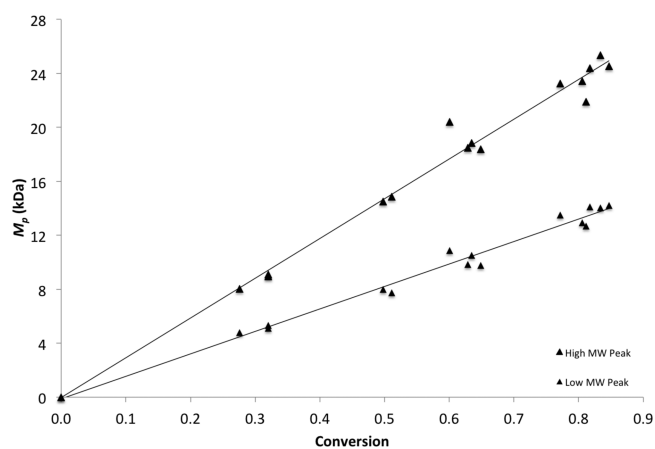


Figure 4. Peak molecular weights (M_p) of each distribution of the bimodal molecular weight distributions produced by the atom transfer radical polymerization of styrene (St) initiated by prop-2-yn-1-yl 2-bromo-2-methylpropanoate (PBiB) at 110 °C as a function of monomer conversion, using N,N,N',N'',N'' -pentamethyldiethylenetriamine (PMDETA) as the ligand; $[St]:[PBiB]:[CuBr]:[CuBr_2]:[PMDETA] = 100:1:1:0.1:1.1$.

radical. We therefore synthesized MBBiB in which chain transfer at the propargylic site is blocked by replacement of the two propargylic hydrogen atoms with methyl groups. When MBBiB was used to initiate the ATRP polymerization of styrene, M_n evolved linearly with conversion (Figure 2), confirming that chain transfer is absent. However, the molecular weights are approximately twice the theoretical values calculated from the initial ratio of the concentrations of monomer to initiator. This corresponds to an *apparent* initiator efficiency of $51 \pm 8\%$ (Table 1). Alternatively, the double molecular weight may be due to a coupling reaction, rather than inefficient initiation, as suggested by the results of the PBiB-initiated polymerizations. In contrast to the PBiB-initiated polymerizations, the molecular weight distributions are monomodal and somewhat narrower ($\mathcal{D} = 1.37$ at 86% conversion vs $\mathcal{D} = 1.46$ at 83% conversion).

The plot of the peak molecular weights for the MBBiB-initiated polymerizations as a function of monomer conversion in Figure 5 is linear, with a slope equal to that of the higher

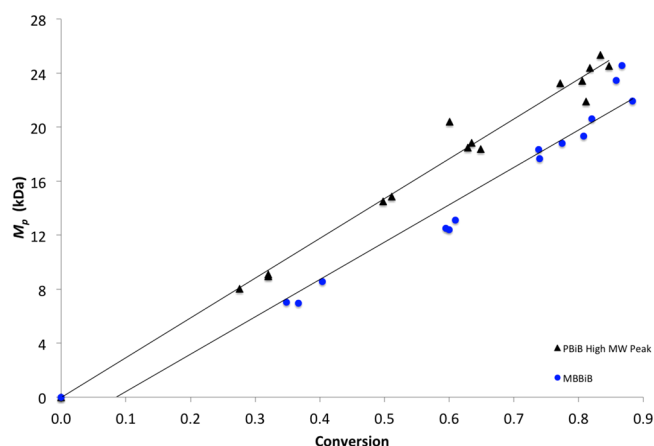


Figure 5. Peak molecular weights (M_p) of the polymers produced by the atom transfer radical polymerization of styrene (St) initiated by prop-2-yn-1-yl 2-bromo-2-methylpropanoate (PBiB; higher molecular weight peak of bimodal distribution in black) and 2-methylbut-3-yn-2-yl 2-bromo-2-methylpropanoate (MBBiB; monomodal distribution in blue) at 110 °C as a function of monomer conversion, using N,N,N',N'',N''' -pentamethyldiethylenetriamine (PMDETA) as the ligand; $[St]:[I]:[CuBr]:[CuBr_2]:[PMDETA] = 100:1:1:0.1:1.1$.

molecular weight distribution from PBiB (Table 1); this also implies that a similar coupling side reaction occurs. Nevertheless, the higher molecular weights and monomodal molecular weight distributions from MBBiB, as exemplified by the GPC traces in Figure 6, suggest that the coupling reaction is much more efficient with MBBiB than with PBiB.³³

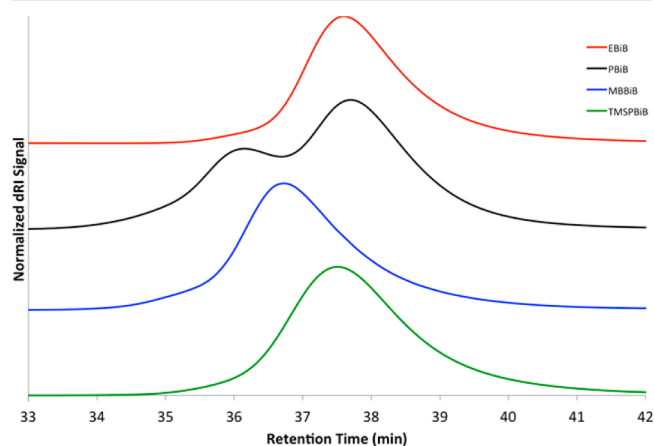


Figure 6. Representative GPC chromatograms at 77–78% conversion of polystyrene initiated from the 2-bromoisobutyrate initiators shown in Scheme 2 at 110 °C using N,N,N',N'',N''' -pentamethyldiethylenetriamine (PMDETA) as the ligand; $[St]:[PBiB]:[CuBr]:[CuBr_2]:[PMDETA] = 100:1:1:0.1:1.1$.

The terminal alkyne position provides another potential site for side reactions (Scheme 1). We therefore synthesized TMSPBiB to block the terminal alkyne site by replacing the hydrogen atom with a trimethylsilyl protecting group. When the ATRP polymerization of styrene was initiated with TMSPBiB (Figure 2), the molecular weight (M_n) increased linearly with conversion, and within experimental error, the apparent initiator efficiency ($75 \pm 5\%$) was equivalent to that of the control initiator ($78 \pm 4\%$) (Table 1). The molecular weight distributions were monomodal and remained narrow ($\mathcal{D} = 1.25$ at 80% conversion) throughout the polymerization,

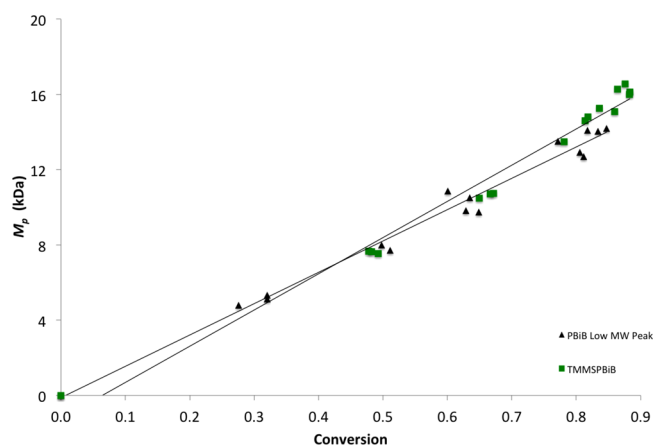


Figure 7. Peak molecular weights (M_p) of the polymers produced by the atom transfer radical polymerization of styrene (St) initiated by prop-2-yn-1-yl 2-bromo-2-methylpropanoate (PBiB; lower molecular weight peak of bimodal distribution in black) and 3-(trimethylsilyl)prop-2-yn-1-yl 2-bromo-2-methylpropanoate (TMSPBiB; monomodal distribution in green) at 110 °C as a function of monomer conversion, using N,N,N',N'',N''' -pentamethyldiethylenetriamine (PMDETA) as the ligand; $[St]:[I]:[CuBr]:[CuBr_2]:[PMDETA] = 100:1:1:0.1:1.1$.

although not as narrow as the control polymerizations ($\mathcal{D} = 1.18$ at 77% conversion). A plot of the peak number-average molecular weights as a function of conversion (Figure 7) is linear, with a slope very close to that of the lower molecular weight distribution from the PBiB-initiated polymerization (Table 1). In contrast to MBBiB with the propargylic site protected, TMSPBiB functions as well as EBiB, the nonalkyne control initiator. Therefore, the dominant side reaction must be alkyne–alkyne coupling, which is suppressed by protecting the acetylenic position with a trimethylsilyl group. In order to confirm this hypothesis, we analyzed the products formed by PBiB and propargyl acetate under ATRP conditions in the absence of monomer.

Model Reaction of PBiB. The possible transfer and termination side reactions of the tertiary radicals generated by PBiB were investigated by monitoring its 1H NMR spectra in benzene- d_6 in the presence of the catalyst system ($CuBr$, $CuBr_2$, and PMDETA) at room temperature and in the absence of monomer. The concentrations and conditions were similar to those used at the beginning of the polymerizations, when the ligand is allowed time to complex the copper halides. As outlined in Scheme 3, the tertiary radical generated by homolytic cleavage of the activated carbon–bromine bond of PBiB may abstract a propargylic hydrogen atom from a second PBiB molecule, followed by quenching of the resulting propargylic radical with cupric bromide to produce prop-2-yn-1-bromo-1-yl 2-bromo-2-methylpropanoate and prop-2-yn-1-yl 2-methylpropanoate. Although abstraction of a propargylic hydrogen atom is favored by resonance stabilization of the resulting propargylic radical, we saw no evidence of this reaction in the PBiB-initiated polymerization of styrene. Similarly, no chain transfer product formed by radical abstraction of a propargylic hydrogen was detected in this model reaction, even after 75 min.

Alternatively, the tertiary radical may react with a second isobutyrate radical by disproportionation to generate prop-2-yn-1-yl methacrylate and prop-2-yn-1-yl isopropanoate, as in the dominant termination mechanism of methacrylate polymerizations (Scheme 2).³⁴ The 1H NMR spectrum in Figure 8

Scheme 3. Chain Transfer vs Termination of the Tertiary Radicals Generated by Activation of Prop-2-yn-1-yl 2-Bromo-2-methylpropanoate under Atom Transfer Radical Polymerization Conditions; PMDETA = *N,N,N',N'',N''*-Pentamethyldiethylenetriamine

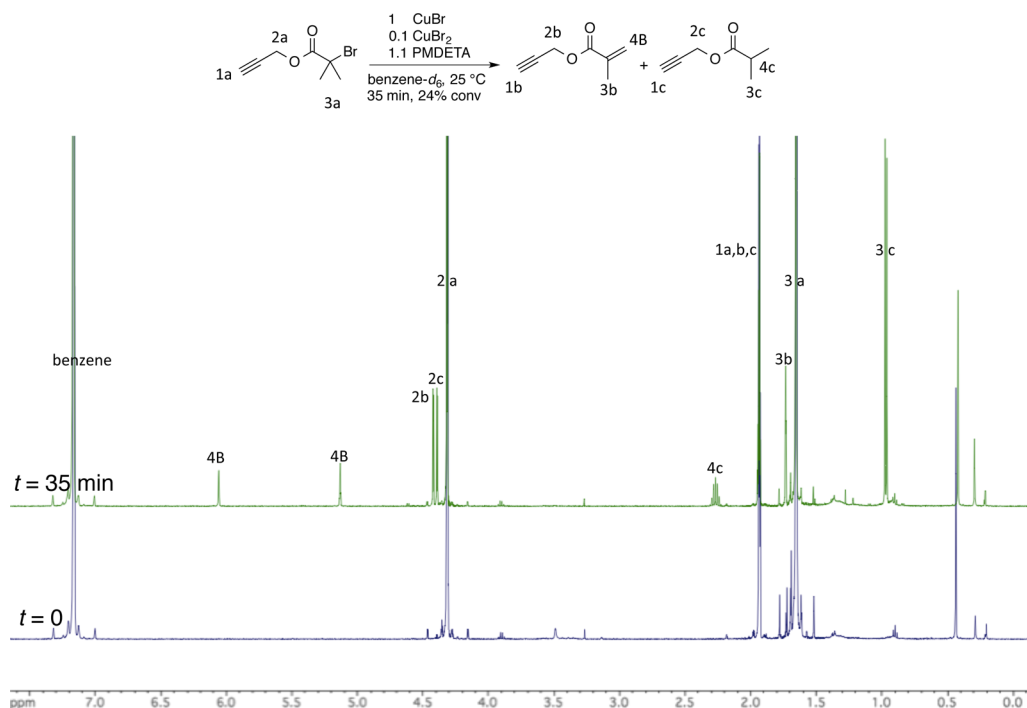
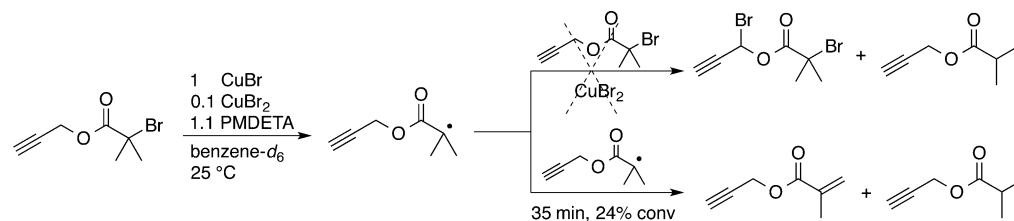


Figure 8. ^1H NMR (500 MHz) spectra of prop-2-yn-1-yl 2-bromo-2-methylpropanoate (PBiB) in benzene- d_6 at 25 °C in the presence of CuBr, CuBr $_2$ and *N,N,N',N'',N''*-pentamethyldiethylenetriamine (PMDETA); [PBiB]:[CuBr]:[CuBr $_2$]:[PMDETA] = 1:1:0.1:1.1.

demonstrates that PBiB generated a substantial amount (24%) of disproportionation products after 35 min under ATRP conditions. This disproportionation side reaction may account for the maximum initiator efficiency of the 2-bromoisobutyrate initiators reported in Table 1, including the control initiator, being only $78 \pm 4\%$.

Model Reaction of Propargyl Acetate. The dominant side reaction in the ATRP polymerizations initiated by PBiB and MBBiB appears to be alkyne–alkyne coupling. Terminal alkynes are rapidly dimerized by oxidative coupling using amine complexes of cuprous halides,^{15–18} which are the most common type of ATRP catalyst systems. These oxidative coupling reactions also require the presence of oxygen or another oxidant; although oxygen should be removed during the extensive degassing procedure, Cu(II) is present in small concentrations throughout the polymerization due to the activation–deactivation equilibrium, and Cu(II) may therefore act as the oxidant in an oxidative coupling reaction.

The possibility of alkyne–alkyne coupling was investigated by monitoring the ^1H NMR spectra of propargyl acetate in benzene- d_6 in the presence of the ATRP catalyst system (CuBr, CuBr $_2$, and PMDETA), first at 25 °C and then at 85 °C. The concentrations and conditions were similar to those used at the

beginning of the polymerizations, although no monomer was present, and the final reaction temperature was lower than that of the polymerization due to the lower boiling point of benzene compared to anisole/styrene. As in the polymerizations, the model reactions were first stirred at room temperature to allow the ligand to form complexes with copper prior to starting the reaction/polymerization. Figure 9 presents the ^1H NMR spectrum of the sample isolated after the initial 30 min at room temperature. New singlet resonances appear at 1.47 ppm and 4.23 ppm due to the formation of the alkyne–alkyne coupled dimer, hexa-2,4-diyne-1,6-diyl diacetate, as confirmed by 2-D gradient heteronuclear multiple bond correlation (gHMBC) NMR spectroscopy (Figure S1 in the Supporting Information).

The amount of this coupled side product (47% conversion after 30 min at 25 °C) did not increase with additional reaction time and heating. (Other side products were detected after 16.5 h at 85 °C but were not identified.) This demonstrates that the oxidant was not present during the reaction, and the small amount of Cu(II) present at equilibrium therefore does not serve as the oxidant for the alkyne–alkyne coupling. Instead, the oxidatively coupled dimer must form when oxygen is present, either when the reactants are mixed together or at the

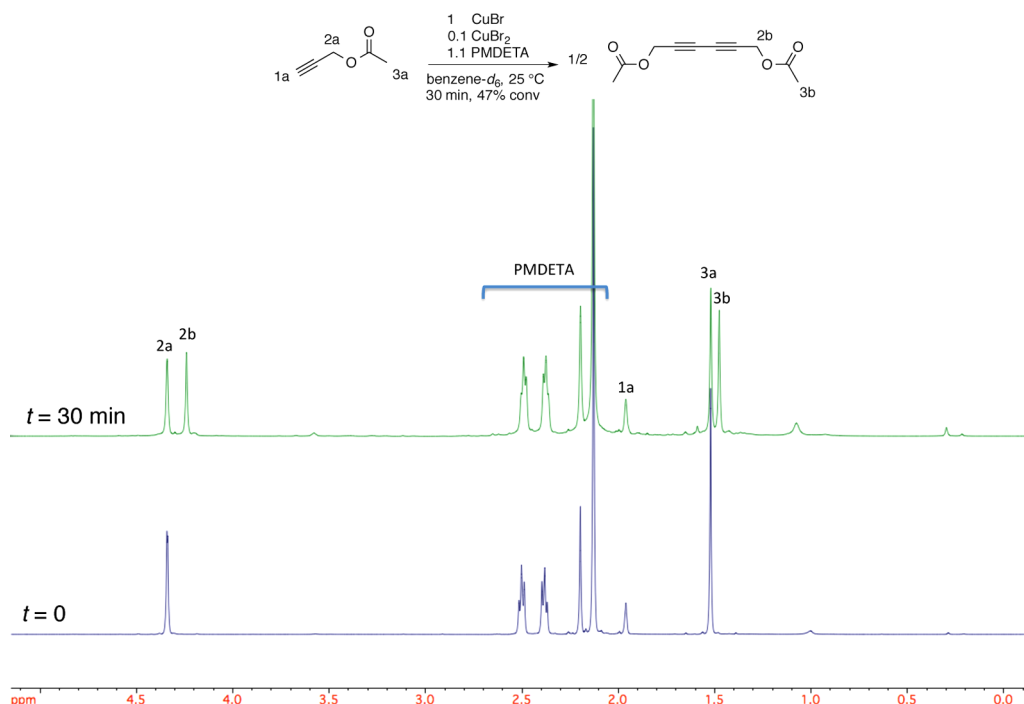


Figure 9. ^1H NMR (500 MHz) spectra of propargyl acetate in benzene- d_6 at 25 °C in the presence of CuBr, CuBr $_2$ and N,N,N',N',N'' -pentamethyldiethylenetriamine (PMDETA); [propargyl acetate]:[CuBr]:[CuBr $_2$]:[PMDETA] = 1:1:0.1:1.1.

end of the polymerization when the polymer is isolated. Since the solution of propargyl acetate and PMDETA was thoroughly degassed by a freeze–pump–thaw technique before adding it to the mixture of CuBr and CuBr $_2$ in a N $_2$ -filled drybox, the most likely time for coupling would have been at the end of the reaction when the products were isolated in air.

CONCLUSIONS

The ATRP polymerizations of 100 equiv of styrene initiated by alkyne-functional initiators in the presence of a CuBr/CuBr $_2$ /PMDETA catalyst system at 110 °C are living, with no detectable termination reactions and no detectable chain transfer reactions, including at the propargylic position, according to first-order monomer conversion plots and molecular weight plots as a function of monomer conversion, respectively. Although the polymerizations initiated by unprotected terminal alkyne-functional initiators are living, the alkyne chain ends undergo oxidative alkyne–alkyne coupling when the polymerizations are exposed to air, and oxygen is introduced in the presence of CuBr/CuBr $_2$ /PMDETA during work-up. This “side reaction” is of significant importance, as it diminishes the orthogonality of CuCAAC/ATRP and the control of ATRP polymerizations. Therefore, in order to produce terminal alkyne-functionalized polymers with controlled molecular weights and narrow polydispersities, the alkyne group must be protected, such as with a trimethylsilyl-protecting group as in the 3-(trimethylsilyl)prop-2-yn-1-yl 2-bromo-2-methylpropanoate-initiated polymerizations.

ASSOCIATED CONTENT

Supporting Information

Synthesis of propargyl acetate and ^1H – ^{13}C gHMBC NMR spectrum of its oxidatively coupled dimer. The Supporting Information is available free of charge on the ACS Publications website at DOI: 10.1021/acs.macromol.5b00652.

AUTHOR INFORMATION

Corresponding Author

*E-mail cpugh@uakron.edu; Tel (330) 972-6614 (C.P.).

Notes

The authors declare no competing financial interest.

ACKNOWLEDGMENTS

Acknowledgment is made to the National Science Foundation for support of this research through DMR-1006195. We also acknowledge Dr. Xiang Yan for synthesizing propargyl acetate.

REFERENCES

- (1) Wang, J. S.; Matyjaszewski, K. *J. Am. Chem. Soc.* **1995**, *117*, 5614–5615.
- (2) Matyjaszewski, K. *Macromolecules* **2012**, *45*, 4015–4039.
- (3) Coessens, V.; Pintauer, T.; Matyjaszewski, K. *Prog. Polym. Sci.* **2001**, *26*, 337–377.
- (4) Zhang, X.; Xia, J.; Matyjaszewski, K. *Macromolecules* **2000**, *33*, 2340–2345.
- (5) Coessens, V.; Matyjaszewski, K. *Macromol. Rapid Commun.* **1999**, *20*, 127–134.
- (6) Mantovani, G.; Ladmiral, V.; Tao, L.; Haddleton, D. M. *Chem. Commun.* **2005**, 2089.
- (7) Lutz, J.-F. O.; Borner, H. G.; Weichenhan, K. *Macromol. Rapid Commun.* **2005**, *26*, 514–518.
- (8) Opsteen, J. A.; van Hest, J. C. M. *Chem. Commun.* **2005**, 57–59.
- (9) Tsarevsky, N. V.; Sumerlin, B. S.; Matyjaszewski, K. *Macromolecules* **2005**, *38*, 3558–3561.
- (10) Ge, Z.; Zhou, Y.; Xu, J.; Liu, H.; Chen, D.; Liu, S. *J. Am. Chem. Soc.* **2009**, *131*, 1628–1629.
- (11) Sumerlin, B. S.; Tsarevsky, N. V.; Louche, G.; Lee, R. Y.; Matyjaszewski, K. *Macromolecules* **2005**, *38*, 7540–7545.
- (12) Ladmiral, V.; Mantovani, G.; Clarkson, G. J.; Cauet, S.; Irwin, J. L.; Haddleton, D. M. *J. Am. Chem. Soc.* **2006**, *128*, 4823–4830.
- (13) Li, Y.; Yang, J.; Benicewicz, B. C. *J. Polym. Sci., Part A: Polym. Chem.* **2007**, *45*, 4300–4308.

- (14) Ladmiral, V.; Legge, T. M.; Zhao, Y.; Perrier, S. *Macromolecules* **2008**, *41*, 6728–6732.
- (15) Hay, A. S. *J. Org. Chem.* **1960**, *25*, 1275–1276.
- (16) Hay, A. S. *J. Org. Chem.* **1962**, *27*, 3320–3321.
- (17) Kennedy, J. C.; MacCallum, J. R.; MacKerron, D. H. *Can. J. Chem.* **1995**, *73*, 1914–1923.
- (18) Siemsen, P.; Livingston, R.; Diederich, F. *Angew. Chem., Int. Ed.* **2000**, *39*, 2632–2657.
- (19) Ciftci, M.; Kahveci, M. U.; Yagci, Y.; Allonas, X.; Ley, C.; Tar, H. *Chem. Commun.* **2012**, *48*, 10252.
- (20) Gregg, R. A.; Mayo, F. R. *J. Am. Chem. Soc.* **1953**, *75*, 3530–3533.
- (21) D'Alelio, G. F.; Evers, R. C. *J. Polym. Sci., Part A-1: Polym. Chem.* **1967**, *5*, 999–1014.
- (22) Zhang, W.; Zhang, W.; Zhang, Z.; Zhu, J.; Zhu, X. *Macromol. Rapid Commun.* **2010**, *31*, 1354–1358.
- (23) Sanchez-Sanchez, A.; Asenjo-Sanz, I.; Buruaga, L.; Pomposo, J. A. *Macromol. Rapid Commun.* **2012**, *33*, 1262–1267.
- (24) Malkoch, M.; Thibault, R. J.; Drockenmuller, E.; Messerschmidt, M.; Voit, B.; Russell, T. P.; Hawker, C. J. *J. Am. Chem. Soc.* **2005**, *127*, 14942–14949.
- (25) Greene, A. C.; Zhu, J.; Pochan, D. J.; Jia, X.; Kiick, K. L. *Macromolecules* **2011**, *44*, 1942–1951.
- (26) Quémener, D.; Davis, T. P.; Barner-Kowollik, C.; Stenzel, M. H. *Chem. Commun.* **2006**, 5051–5053.
- (27) Eugene, D. M.; Grayson, S. M. *Macromolecules* **2008**, *41*, 5082–5084.
- (28) Zhang, W.; Müller, A. H. E. *Polymer* **2010**, *51*, 2133–2139.
- (29) Dimitrov, I.; Takamuku, S.; Jankova, K.; Jannasch, P.; Hvilsted, S. *Macromol. Rapid Commun.* **2012**, *33*, 1368–1374.
- (30) Chen, G.; Tao, L.; Mantovani, G.; Ladmiral, V.; Burt, D. P.; Macpherson, J. V.; Haddleton, D. M. *Soft Matter* **2007**, *3*, 732–739.
- (31) Hwu, J. R.; Furth, P. S. *J. Am. Chem. Soc.* **1989**, *111*, 8834–8841.
- (32) Tsarevsky, N. V.; Sumerlin, B. S. *Fundamentals of Controlled/Living Radical Polymerization*; Royal Society of Chemistry: London, 2012.
- (33) Note that the initiator efficiency reported in Table 1 for PBiB is based on M_n for the bimodal molecular weight distribution.
- (34) Odian, G. *Principles of Polymerization*, 4th ed.; Wiley-Interscience: New York, 2004.